Expression of Cell-Adhesion Molecules in Embryonic Induction. II. Morphogenesis of Adult Feathers

CHENG-MING CHUONG and GERALD M. EDELMAN
The Rockefeller University, New York, New York, 10021

ABSTRACT The developmental appearance of cell-adhesion molecules (CAMs) was mapped during the morphogenesis of the adult chicken feather. Neural CAM (N-CAM), liver CAM (L-CAM), and neuron-glia CAM (Ng-CAM), as well as substrate molecules (laminin and fibronectin), were compared in newborn chicken skin by immunohistochemical means. N-CAM was found to be enriched in the dermal papilla, which was closely apposed to L-CAM–positive papillar ectoderm. The two CAMs were then co-expressed in cells of the collar epithelium. Subsequently generated barb epithelia expressed only L-CAM, but N-CAM reappeared periodically on cells between developing barbs and barbules. N-CAM first appeared on a single L-CAM–positive basilar cell located in each valley flanked by two adjacent barb ridges. Subsequently, the expression of N-CAM extended one cell after another to include the whole basilar layer. N-CAM also appeared in the L-CAM–positive axial-plate epithelia, beginning in a single cell located at the ridge base. The two collectives of N-CAM–positive epithelia constituting the marginal and axial plates then disintegrated, leaving interdigitating spaces between keratinized structures that had previously expressed L-CAM. The morphological transformation from an epithelial cylinder to a three-level branched feather pattern is thus achieved by coupling alternating CAM expression in linked cell collectives with specific differentiation events, such as keratinization. During all of these morphogenetic processes, laminin and fibronectin formed a continuous basement membrane separating pulp from feather epithelia, and were excluded from the sites involved in periodic appearances of N-CAM. The same staining pattern described for developing chickens persisted in the feather follicles of adult chicken tissue that have gone through several cycles of molting. Cyclic expression of the two different CAMs underlies each of the different morphological events that are generated epigenetically during feather morphogenesis.

During development, the morphogenesis of tissues and of the whole animal is achieved by means of differential regulation of a series of epigenetic sequences consisting of such primary processes as cell division, movement, death, adhesion, and differentiation (1–3). It has been suggested (4) that modulation of cell adhesion plays a particularly important regulative role in these sequences by linking epithelia, creating mesenchyme, and altering morphogenetic movements. Previous studies (reviewed in references 5–7) have led to the identification of two primary cell-adhesion molecules (CAMs),[1] the neural CAM (N-CAM) (8), and the liver CAM (L-CAM) (9), as well as one secondary CAM, the neuron-glia CAM (Ng-CAM) (10). The regular expression of primary CAMs at sites of embryonic induction, such as the neural plate, several placodes, the limb bud, and kidney (11–13), suggested that the proximity of collectives of cells linked by N-CAM to those linked by L-CAM (CAM couples) may play a role in the control of the milieu-dependent differentiation that follows inductions.

Feather morphogenesis provides a particularly good opportunity to study this process because, in development, centers of feather induction exist in large numbers on the chicken skin at different stages of progession (14, 15). In our companion paper (16), we described studies on the expression of CAMs during the histogenesis of nestling feathers. We found that N-CAM/L-CAM couples occur at each feather placode, that adhesion mediated by N-CAM most likely helps to

[1] *Abbreviations used in this paper:* CAM, cell-adhesion moleule; L-CAM, N-CAM, and Ng-CAM, liver, neural, and neuron-glia CAM, respectively; SAM, substrate-adhesion molecule.

mediate dermal condensation, and that N-CAM is assymmetrically localized in the dorsal portion of the feather bud dermis. Later, N-CAM was shown to appear periodically in cells located in the valleys between successive L-CAM–positive barb ridges. These findings are consistent with the idea that modulation of CAM expression at each morphogenetic site is important in forming periodic feather patterns.

In the present study, we analyze the adult feather, which differs from the radially symmetric nestling feather in showing bilateral symmetry with respect to a rachis (15, 17). With the formation of the rachis, another level of complexity affecting feather pattern, shape, and size is added to the morphogenetic schedule that leads to this skin appendage (15). Moreover, feather molting cycles occur throughout adult life (15, 18). It is, therefore, particularly important to examine further how the more complex patterns of the adult feather are achieved, and to assess whether the appearance of CAM couples is included in the repetitive events that lead both to new feathers and to new parts of feathers. The results of these studies show a remarkable pattern of appearance of CAM couples that appear periodically at each branching point and each level of feather pattern formation.

MATERIALS AND METHODS

The methods used were the same as those described in the accompanying paper (16). Briefly, White Leghorn chicken skin (from spinal tract on the back or from the ulnar side of the alar tract on the wing) was fixed by 2.5% paraformaldehyde/0.02% glutaldehyde in PBS and 10-μm frozen sections were prepared. The sections were reacted with anti-N-CAM (8, 19), anti-L-CAM (9), anti-Ng-CAM (10), antifibronectin (cellular form) (gift of J.-P. Thiery, Institut d'Embryologie du Centre National de la Récherche Scientifique et du Collège de France), and antilaminin (E.-Y. Lab, San Mateo, CA); in each case the treated sections were then incubated with appropriate fluorescent secondary antibodies (Miles Laboratories, Nagerville, IL).

RESULTS

In the first two months of life, the nestling feathers of the chicken are gradually replaced by adult feathers in the process called molting (15). We correlated the histogenesis of these adult feathers with the distribution of CAMs (L-CAM, N-CAM, and Ng-CAM) and of fibronectin and laminin. Both of the latter are components of the extracellular matrix (21) and are referred to here as substrate-adhesion molecules (SAMs). The terminology used for the feather structures is illustrated in the diagram in Fig. 1*A*.

Early Steps in Adult Feather Development

NEWLY HATCHED CHICKEN SKIN: After hatching, nestling feathers are present on the skin, and adult feathers have started to form in their follicles. Eventually, the adult feathers replace the nestling feathers, pushing them outward (15). Because this molting process occurs in waves for different feathers and because of the occurence of feather varieties, the different pterylae of newly hatched chicken skin show different types and different stages of developing adult feathers (15). There are two major morphogenetic steps in adult feathers that differ from nestling feathers (15, 17): (*a*) the great increase in the number and size of barb ridges affecting the size and shape of the feather; (*b*) the formation of the rachis with accompanying changes in symmetry of the feather from radial to bilateral. In keeping with these changes, staining with anti-CAM antibodies reveals a much more complex periodic pattern than that seen in the development of nestling feathers. First, we will consider the fundamental early events, and then discuss the differences between the development of nestling and adult feathers as they bear upon CAM expression.

DERMAL PAPILLA AND EPIDERMAL COLLAR: Dermal papillae, which originate from the dermal condensations, became biconvex-shaped structures that are situated periodically in the dermis. They are formed by closely compacted cells that were found to be highly N-CAM–positive (Fig. 1 *B, a'*), but negative for L-CAM (Fig. 1 *B, a*), fibronectin (16), and laminin (not shown). The L-CAM–positive epidermis has invaginated from the skin surface to become the follicular wall, and after reaching the follicular base, forms a 180° turn to become the papillar ectoderm that wraps around the dermal papilla (14, 15). It then becomes the cylindrically shaped epidermal collar that is a site of active mitosis (14, 15); cells in the collar were found to be both L-CAM– and N-CAM–positive (Fig. 1 *B, c* and *c'*). The newly generated cells are pushed upward and are segregated into a single cell thick basilar layer lying between the pulp cavity and the barb-ridge epithelium. During development, cells in the basilar layer showed a decrease in L-CAM staining and an increase in N-CAM staining; in contrast, cells in the barb-ridge epithelium showed a decrease in N-CAM while remaining L-CAM–positive (Fig. 1 *B, b* and *b'*). Because new cells are inserted successively in the base of the feather, there is a maturation gradient from the base to the tip (15, 17), and successive sections of the shaft show sequential stages of barb-ridge development as described below.

Intermediate Steps in Adult Feather Development

BARB RIDGE, BASILAR LAYER, AND AXIAL PLATE: The process of barb-ridge formation (15) involves events that morphologically transform an epithelial cylinder into a highly elaborated feather structure with three levels of branching. For clarity, the correlated chronological events of barb-ridge formation and of CAM and SAM expressions to be described are shown schematically in Fig. 2 before presenting the data in detail. Because of the complexity of the pattern, we summarize here the principles governing this developmental sequence. The general principles are the following: (*a*) events occur one after another following an exact sequential order; (*b*) once initiated, each event follows a similar propagation pattern in three maturation gradients: from the tip to base along the longitudinal axis of the feather, from the dorsal to the ventral side in the cross section of the feather (the dorsum is defined as that side containing the rachis), and from the base to tip along each barb-ridge axis; (*c*) inasmuch as an early event is the invagination of the epithelial cylinder to form many barb ridges, all subsequent events show a periodic pattern; (*d*) the arrangement of the L-CAM–positive epithelia into structures reflecting barb and barbule formation is coupled with the appearance of N-CAM–positive cells in specific alternating positions within these structures; (*e*) epithelial cells expressing N-CAM follow differentiation pathways distinct from cells expressing L-CAM: instead of keratinizing into permanent structures, as did the L-CAM–positive cells, N-CAM–positive cells disintegrated, leaving spaces between the keratinized structures. Separation of barbs and barbules appears to be the consequence of the death of these N-CAM–containing cells.

Barb-ridge formation (Fig. 3, *a* and *a'*) was followed by the first wave of N-CAM appearance between two ridges (Fig. 3,

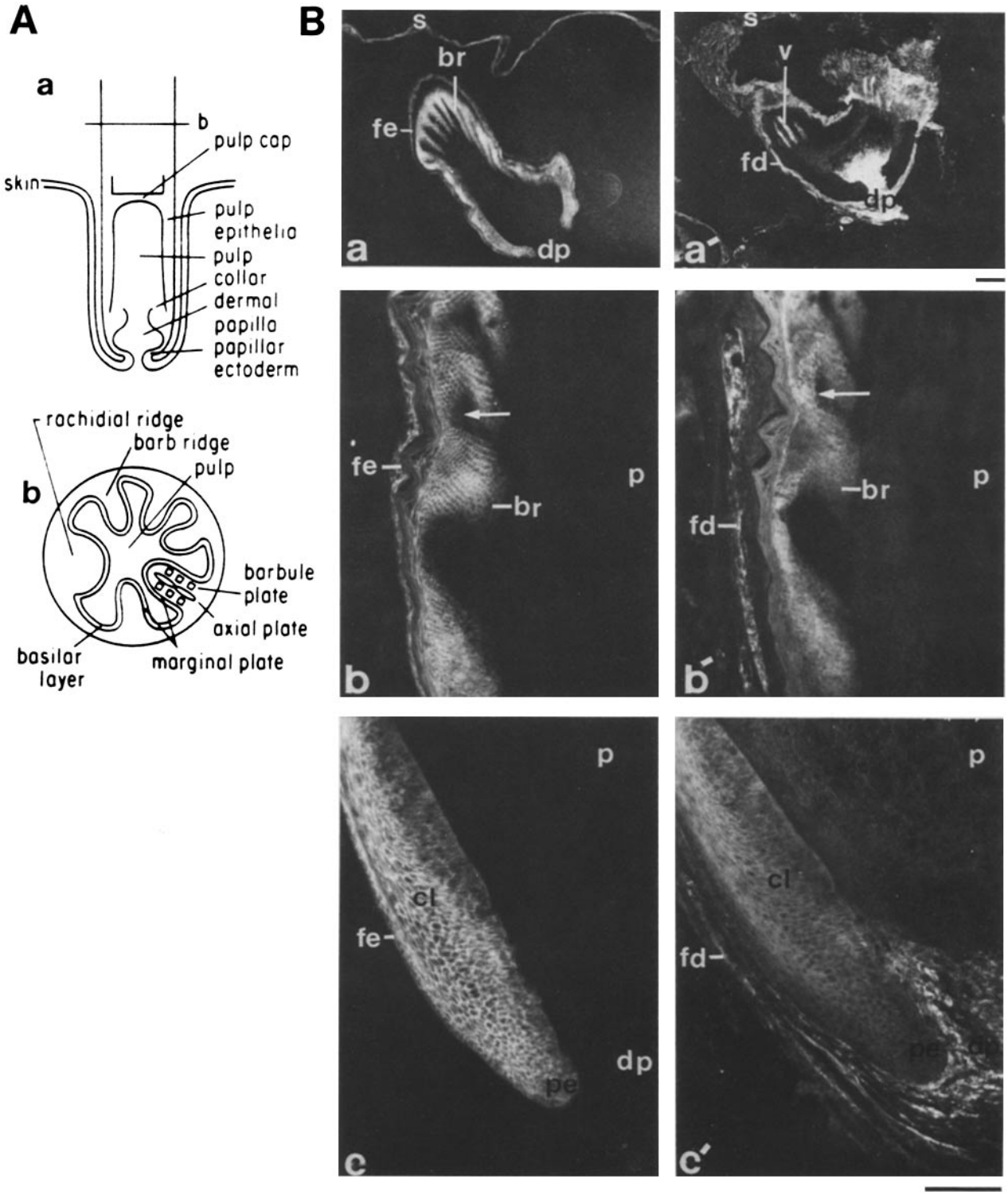

FIGURE 1 (*A*) Schematic drawing of a developing adult feather illustrating the terminology used. (*a*) Longitudinal section. (*b*) Cross section at the level indicated in *a*. (*B*) Dermal papilla and epidermal collar. Longitudinal sections of feather follicles from the wing of a 2-wk-old chicken stained with anti-L-CAM (*a*–*c*) and anti-N-CAM (*a'*–*c'*). (*a* and *a'*) A developing follicle showing a dermal papilla (*dp*) positive for N-CAM, while barb ridges (*br*) are stained with L-CAM in an alternating fashion. Follicular epidermis (*fe*) is positive for L-CAM while follicular dermis (*fd*) is positive for N-CAM. *s*, skin; *v*, valley between barb ridges. (*b*, *b'*, *c*, and *c'*) Dermal papilla and epidermal collar; the views show double staining of portions of a developing follicle. The papillar ectoderm (*pe*) is L-CAM–positive, the dermal papilla (*dp*) is N-CAM–positive, and the collar (*cl*) is both L- and N-CAM–positive. The N-CAM staining is absent in the epithelial cells of the barb ridge (*br*) but is accentuated in the basilar layer over the valley (arrow). Also note the well organized lattice structure made up of barb epithelial cells. *p*, pulp cavity. Bars, 100 μm. (*a* and *a'*) × 50. (*b*–*c'*) × 126.

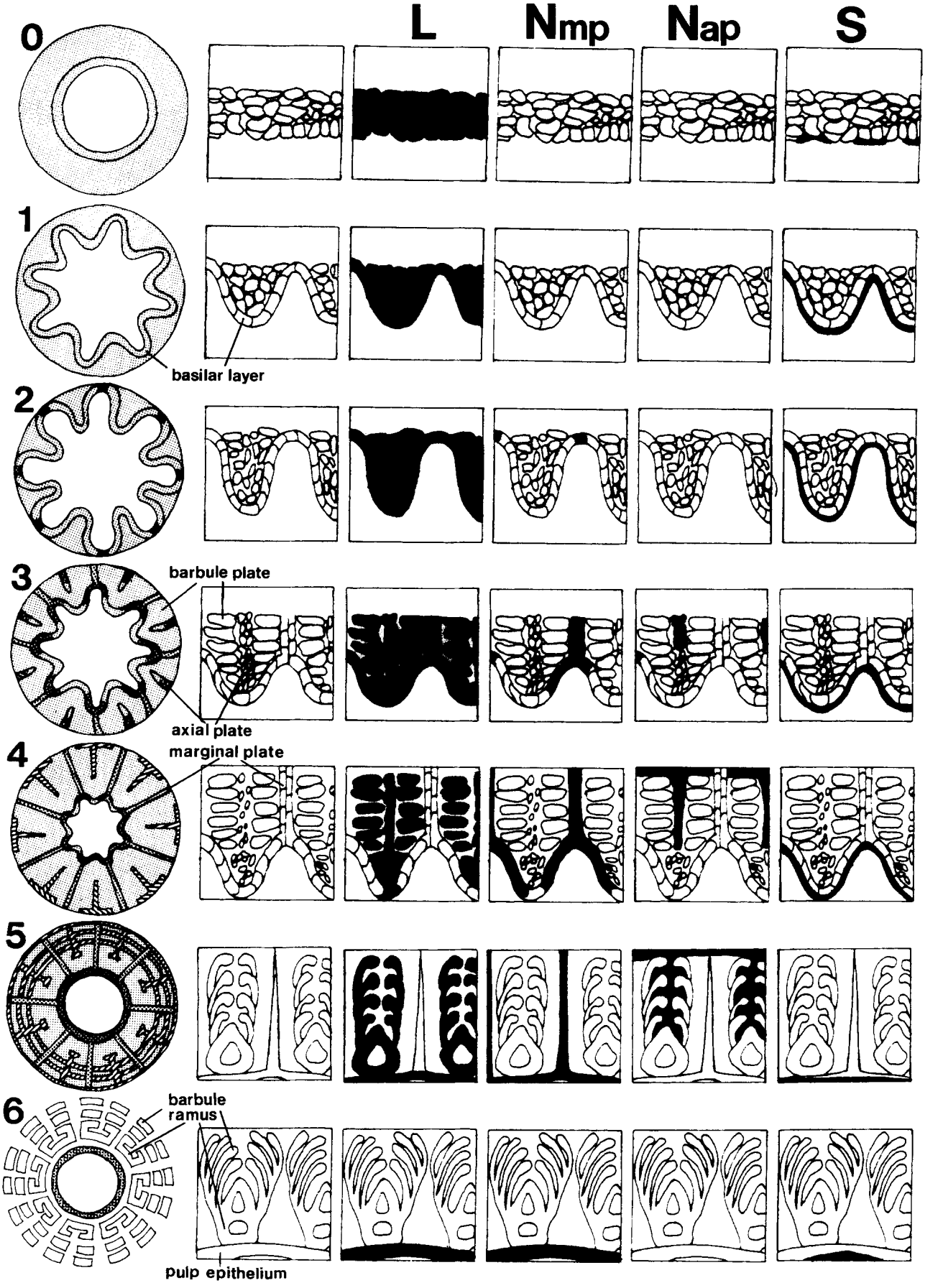
L
Nmp
Nap
S
0
1
basilar layer
2
3
barbule plate
axial plate
4
marginal plate
5
6
barbule
ramus
pulp epithelium

b and *b'*). Later events of barbule-plate formation were followed by a second wave of N-CAM appearance (Fig. 3, *c* and *c'*) in the axial-plate cells between each of two rows of barbule-plate cells. As indicated by the curved solid arrows in Fig. 3, *a*, *a'*, and *b*, the fronts of two barb ridge–forming waves can be seen to extend bilaterally and ventrally, eventually meeting in the ventral point of the feather (from *a* to *a'* to *b* to *b'* in Fig. 3). N-CAM staining was observed in a periodic pattern increasing in intensity from the ventral to the dorsal side (Fig. 3, *b* and *b'*, curved blank arrow); this paralleled the dorsoventral maturation gradient that has been described for barb ridges (15, 16). The expression of CAMs at the cellular level is shown in Figs. 4 and 5. N-CAM was first expressed in a single cell of the basilar layer in the valley between two ridges. This expression then extended bilaterally toward the ridge tips, forming a "U" shaped staining pattern (Fig. 4, *b'* and *c'*). N-CAM–positive cells from the bottom of the "U" then are rearranged, "zipping" in to form a Y-shaped marginal plate (Fig. 4*d'*); at later times, when this process reached the ridge tip, a "T" shaped staining pattern was seen (Figs. 3*d* and 5*b'*). Cells in the vertical long arm of the "T" ultimately disintegrated, leaving the barb septum that remained N-CAM–positive; cells in the short cross bar of the "T" are linked (Figs. 3*e* and 5*c'*) to form the pulp epithelium (see Fig. 2 for summary).

At the same time as these events take place, epithelial cells generated from the ramogenic column in each barb-ridge tip are organized into two rows of rectangular barbule-plate cells with the spindle-shaped axial-plate cells in between (Fig. 4, *a–d*). The second wave of N-CAM appearance started in one cell of the axial plate located at the base of the ridge, then extended onto adjacent cells toward the ridge tip, forming an I-shaped staining pattern (Fig. 4*d'*). Gradually, this successive appearance of N-CAM began to branch into the periphery of the barb base, eventually forming a set of "T" shaped staining patterns that were in reverse orientation with respect to those seen in the barb septa. The short arms of the "T" eventually fused to form a continuous membrane concentric and peripheral to the pulp epithelium (Figs. 3*d* and 5*b'*); cells in the long arm of the "T" disintegrated to leave the branching pattern of N-CAM staining in between the barbule plates, a residue that eventually comprises a tree-like (Fig. 5*b'*) staining pattern. (See Fig. 2 for summary.)

While these particular epithelial cells are expressing N-CAM, keratinization has begun in the rest of the epithelia made up of L-CAM–positive cells in an order following the same maturation gradient (20). These keratinizing cells eventually become the permanent structures of the feather; the spaces in between result from the death of the N-CAM–positive cells. This selective death completes the morphogenetic process from an epithelial cylinder into the highly elaborated feather structure.

THE RACHIDIAL RIDGE AND THE CHANGE FROM RADIAL TO BILATERAL SYMMETRY: A nestling feather contains 8 to 15 barbs that are radially inserted at the same level on the calamus; in contrast, an adult feather can contain up to several hundred barbs that are bilaterally inserted at different levels on the rachis (15). During formation, the valleys between barb ridges extend away from the rachidial ridge at a 30° angle distally and laterally, like an opening slit. As in barb-ridge formation, there are two waves of N-CAM expression. The first one, in the basilar layer, initiates from the base of the developing valley and extends toward the junction with the rachidial ridge; the second wave, seen in the cells of the axial plate, initiates at the tip of the developing feather and extends toward the base (Fig. 6, *a'*, *b'*, and *c'*). Thus, in longitudinal sections, the observed order of N-CAM appearance proceeds from the feather tip toward the feather base (Fig. 6*b'*); another gradient from the ridge base to the tip is observed in the cross sections of the feathers (summarized in Fig. 2).

During these morphogenetic processes, extracellular substrate molecules (21), such as fibronectin and laminin, are expressed at the boundary between the pulp and epithelium without showing the dynamic changes observed for N- and L-CAM (Fig. 6*a''*). These SAMs appeared first only in the pulp, then on the pulp side of the basilar layer, and, finally, were excluded from the barb septum to lie on the pulp side of the pulp epithelium (see Fig. 3*e''*).

The specificity of N-CAM staining on the epithelia originating from the basilar layer and the dermal papilla was confirmed by the observation that several specific monoclonal antibodies yielded the same staining pattern. Moreover, the staining by polyclonal antibodies to N-CAM was completely neutralized by affinity-purified brain N-CAM (Fig. 6*d*).

Late Steps in Adult Feather Development

RACHIS AND OTHER KERATINIZED STRUCTURES: During development of the rachis, cells in the rachidial ridge were at first positive for both L- and N-CAM; but they soon segregated into three layers: the outermost layer continued to express both CAMs, the middle layer showed only N-CAM,

FIGURE 2 Schematic representation of stages of barb-ridge formation (15, 17) correlated with L- and N-CAM appearance. Stages are arbitrarily chosen for convenience in description. This figure illustrates the cleavage of an epithelial cylinder into a highly elaborate feather in which numerous small barbules (tertiary branches) are connected to rami (secondary branches), and these in turn are connected to the rachis (primary branch) or calamus (not shown). Cross sections of a whole feather are on the left; those of a single barb ridge are on the right. In the sections of whole feather, L-CAM (*L*) is shown as small dots; the first wave of N-CAM appears in the marginal plate (*Nmp*) and is represented as large dots; the second wave of N-CAM appears in the axial plate (*Nap*) and is shown as cross hatches. On the sections of barb ridges, black shadows indicate the presence of each molecule. *S*, substrate adhesion molecules, shown here are fibronectin and laminin. In each stage, events occur in the order given. Stage 0: (*i*) Production of stratified epithelia; (*ii*) initiation of basilar layer formation. Stage 1: initiation of cleavage to form barb ridges; the basilar layer well formed. Stage 2: initiation of a barbule-plate formation; initiation of axial-plate formation; mitosis in the tip of the ridges. Stage 3: marginal plates formed; barbule plates well-formed. Stage 4: widening of barbule-plate cells; arrest of mitosis. Stage 5: barbule-plate cells curve into a comma shape; ramogenic cells vacuolate to form the medulla of the ramus; both start to keratinize. Stage 6: keratinization completed; separation of structures. The numbers and sizes of each structure are schematic and do not reflect the actual values. (For background, see references 15, 17.)

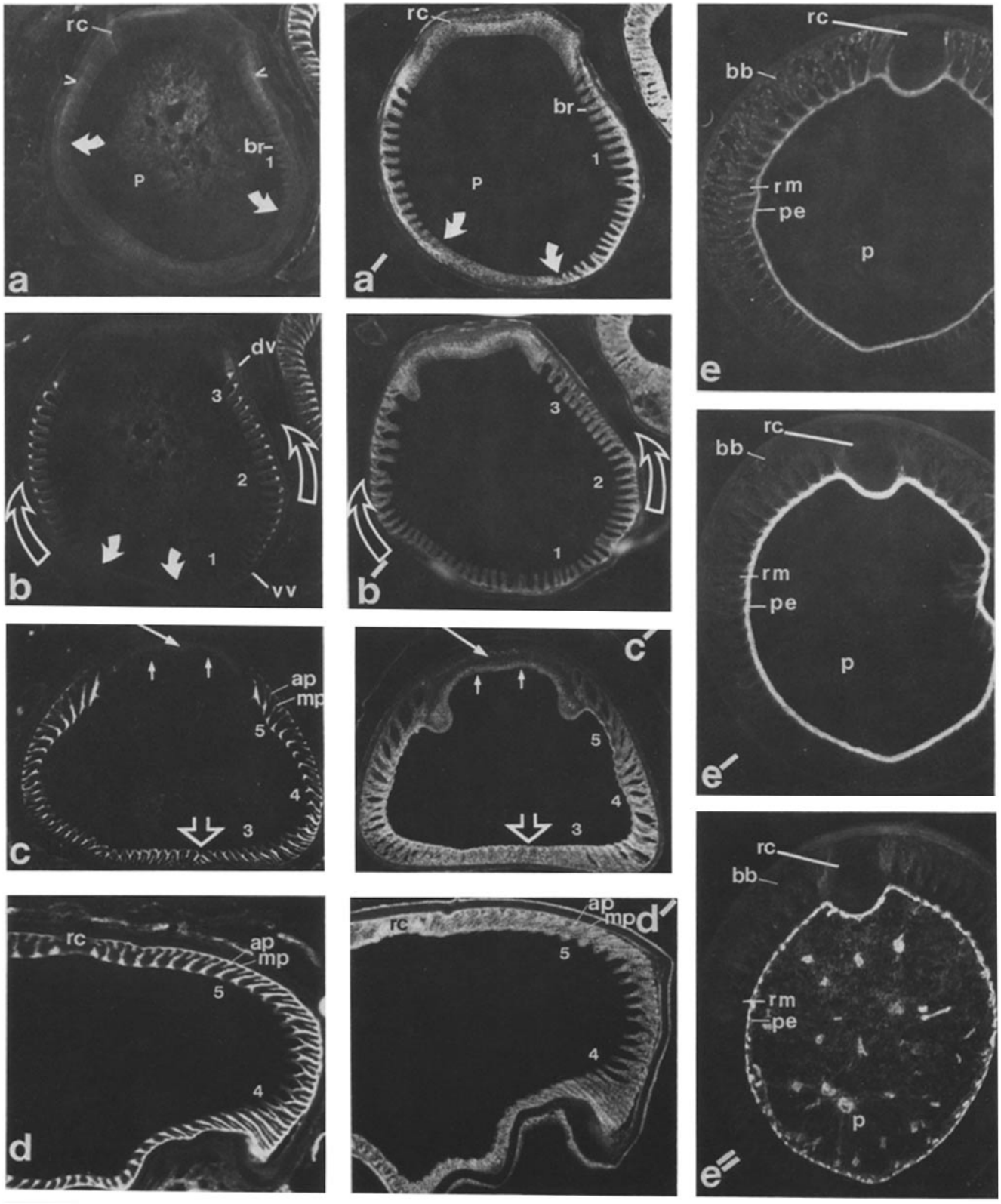
rc
br
1
P
a
a'
dv
3
2
1
vv
b
b'
ap
mp
5
4
3
c
c'
d
d'
bb
rm
pe
p
e
e'
e''

and the inner layer showed only L-CAM (Figs. 3, *a–c′*, and 7 *a*). The rachidial ridge contains small ridges that have a corresponding enlarged middle layer (Fig. 7, *a* and *a′*). Again, unlike the CAMs, fibronectin and laminin were found on the pulp side of the innermost epithelial layer but not within the rachidial ridge (not shown).

In later stages, all of the cells underwent keratinization as the L-CAM–positive cells in the middle of the rachis vacuolated to form the medulla. On the barb ridge, mitosis increases within the ramogenic column at the tip, and cells of the column vacuolate and keratinize to form the ramus (15). The rectangular barbule-plate cells change into cells having a "comma" shape with stalks pointing toward the direction of the ramus (Fig. 5 *b″*). The L-CAM between neighboring barbule cells in the same cross-sectional plane was gradually lost as N-CAM appeared in this space (Fig. 5, *b* and *b′*). After keratinization, cells in the barbule are linked to the ramus through their lower ends, but are free from connections on all other surfaces that previously contacted N-CAM. After all of the N-CAM–positive structures disintegrated, leaving spaces between the epithelial cylinder (Fig. 5, *b–c″*), the elaborated feather emerged: the rachis is the primary branch inserted on the skin, the ramus is the secondary branch inserted on the rachis and the barbule is the tertiary branch inserted on the ramus (Figs. 3–7).

The feather sheath, which originates from a stratified, epithelial layer peripheral to the barb ridges, also keratinizes and will flake off when the feather grows out (15). The proliferative collar keratinizes into the calamus (into which the rachis inserts), and the invaginated skin that surrounds the feather has become the follicular wall, which is composed of epidermis and dermis (15). The germinal layer of the follicular epidermis was L-CAM–positive (Fig. 8, *a* and *c*), but the keratinized corneum layer was negative. The follicular dermis, a thin line of cells closely apposed to the epidermis, remained N-CAM–positive (Fig. 8, *b* and *d*); it is at this place that the muscle is inserted.

PULP, PULP EPITHELIUM, AND DERMAL PAPILLA: The pulp, which is the main nutritive organ of the feather, is positive for fibronectin and laminin, and contains nerves that were Ng-CAM–positive (Fig. 6 *e*). It is surrounded by the pulp epithelium, which was both N- and L-CAM–positive (Fig. 7, *f–g′*). When the feather is keratinized, the pulp is reabsorbed in stages from the tip toward the base, together with the pulp epithelium (Fig. 7 *d*) that retreats with the stepwise formation (15) of pulp caps (Fig. 7 *e*). The degeneration of pulp epithelium above the pulp cap marks the disappearance of the pulp cavity and the full release of the barbs.

Dermal papillae were found to remain N-CAM–positive in the fully grown (6-mo-old) chicken. Molting, which is a repetition of the same feather histogenetic process described above, takes place at a cycle of ~3 mo (15) and needs the interaction of epidermis with the dermal papilla (15, 17). Active barb-ridge formation with typical N-CAM staining (Fig. 7, *h* and *i*) and L-CAM (not shown) staining was observed in the follicles of the adult chicken.

A global view of the appearance of CAMs on a whole developing feather follicle is seen in the sagittal sections shown in Fig. 8, *a–d*.

DISCUSSION

The present correlation of the sites of appearance of CAMs and SAMs with the morphogenetic processes that yield the adult feather indicates that a general aspect of feather formation is the periodic appearance of two adjoining collectives comprising cells that are separately linked within each collective by a different primary CAM. Such CAM couples were observed at every level of morphogenetic expression from the formation of the feather bud through the final formation of barbules. The main findings that support this conclusion are the following: (*a*) Pattern forming events occur in a definite sequence in which the L-CAM–positive barb ridges alternate with the N-CAM–positive marginal plates. This is followed by alternation of the L-CAM–positive barbule plates with the N-CAM–positive axial plates. It is important to note that the patterned cellular geometry of L-CAM–containing cells precedes the periodic appearance of N-CAM. (*b*) In a morphogenetic process resembling the lost wax method of sculptural casting, the cell collectives in the marginal and axial plates that express the N-CAM later disintegrate to leave interdigitating spaces between the cell collectives expressing L-CAM, which themselves keratinize to become feather structures. Successive correlations of CAM expression with those differentiation events results in the branching feather patterns. (*c*) SAMs do not appear to play the same regulatory role in morphogenetic pattern formation as CAMs. Laminin and fibronectin were found in a continuous and homogenous

FIGURE 3 Barb-ridge formation (15, 17), low power view. Sections of wing skin from a 5-wk-old chicken showing cross sections of developing feather from early to late stages (in order from *a* to *e*) stained with anti-N-CAM (*a–e*), anti-L-CAM (*a′–e′*), and antifibronectin (*e″*). The formation of the barb ridges (*br*) starts from the dorsal side (the side with the rachis) and progresses bilaterally toward the ventral side, making a ventrodorsal maturation gradient. Positions of the last formed ridges are marked by curved arrows, and the distance between these two arrows narrows from *a* to *a′* to *b* as the feather matures. The two ridge-forming waves meet on the ventral side (indicated by the blank arrow in c). Numbers designate the stages of barb ridge formation as shown in Fig. 2. (*a* and *a′*) The stratified feather epithelium has just started to form the barb ridges. It is mainly L-CAM–positive; some regions (extensions of the collar) also express faint N-CAM staining (arrowhead). *p*, pulp cavity; *rc*, rachidial ridge. (*b* and *b′*) Bright N-CAM staining starts to appear in the valleys between pairs of the barb ridges. N-CAM appearance starts about eight ridges away from the last formed ridge (*vv*, ventral valley) and increases in staining intensity and distribution dorsally (*dv*, dorsal valley) until it reaches the rachis (curved blank arrows point to the direction of maturation). (*c–d′*) N-CAM staining appears alternately in the marginal plates (*mp*); axial plates (*ap*) are seen at different maturation stages (see Fig. 2 for the stage numbers). On the rachidial ridge, cells lining the pulp cavity are L-CAM–positive but N-CAM–negative (small arrows); the cells peripheral to them are weakly N-CAM–positive but L-CAM–negative (big arrow). (*e* and *e′*) Parts of the basilar layer are linked to form a continuous pulp epithelium (*pe*), that is both N-CAM– (*e*) and L-CAM–positive (*e′*). The barb ridge has keratinized into barbules (*bb*) and ramis (*rm*). (*e″*) Antifibronectin staining at the same stage. Fibronectin is on the basement membrane that lines the pulp side of the pulp epithelium (*pe*) and is in the pulp mesenchyme (*p*). Bar, 100 μm; × 50.

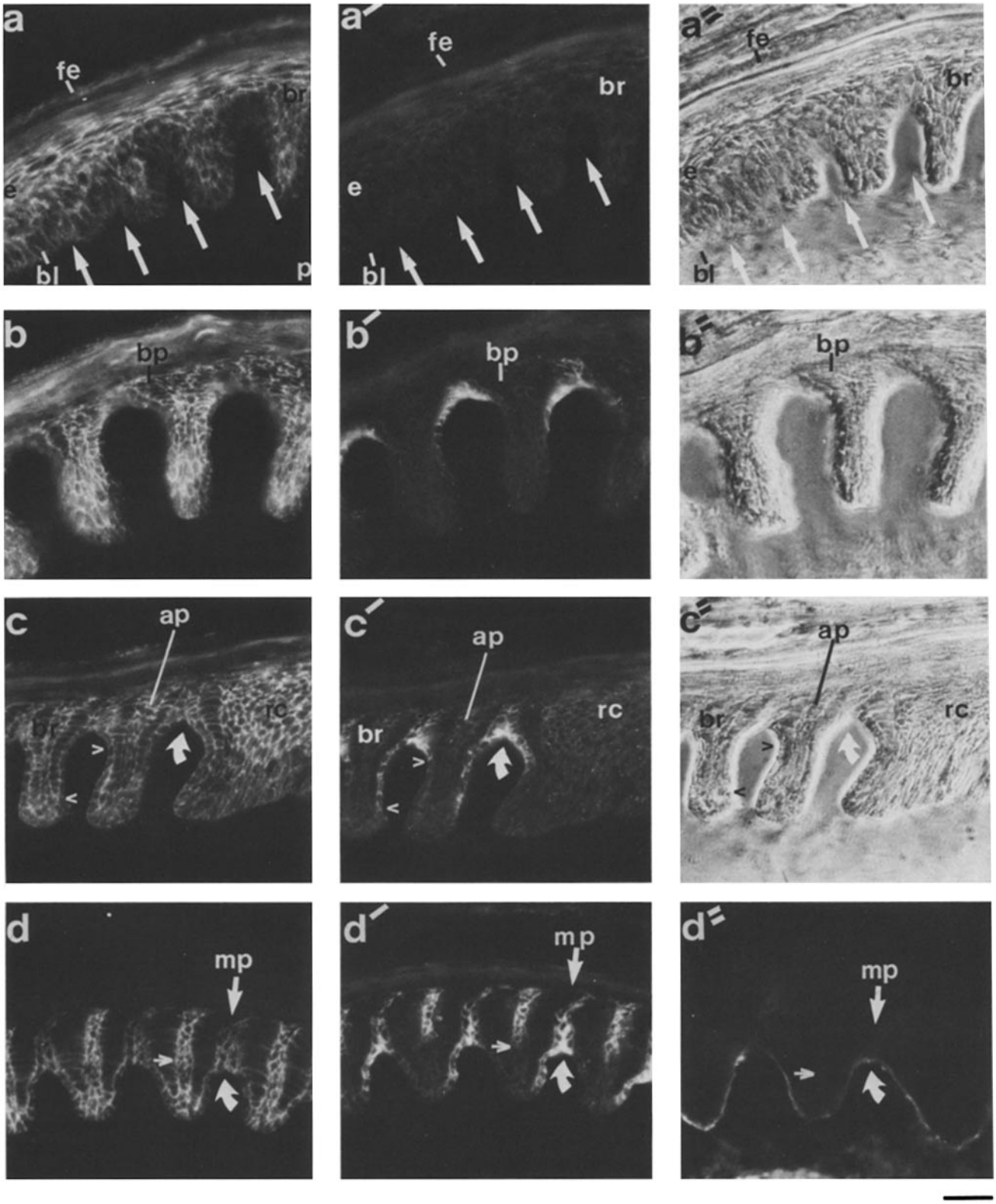
a
fe
br
e
bl
p
a'
fe
br
e
bl
a''
fe
br
e
bl
b
bp
b'
bp
b''
bp
c
ap
rc
br
c'
ap
rc
br
c''
ap
br
rc
d
mp
d'
mp
d''
mp

basement membrane outside the basilar layer and the axial plate, and not at the sites at which periodic and dynamic expression of N-CAM takes place. (*d*) The CAM expression sequence is not unique to feather patterns, but is also seen at many induction sites such as limb buds, placodes, and kidneys (11–13, 22).

Using this background and that provided by the preceding paper (16), we shall discuss the mapping of CAM expression onto the lineages of cells used in feather histogenesis (15), consider periodic pattern formation within a single feather, compare the different morphogenetic functions of CAMs and SAMs, and finally touch upon the possible part played by epigenetic CAM cycles in morphogenesis.

Mapping of CAM Expression on Lineages of Feather Cells

N- and L-CAM both are expressed on single cells of the blastoderm (12). After neural induction, the two CAMs become segregated: L-CAM is found on all the epithelia (ectoderm, endoderm, and some mesoderm), while N-CAM is found on all neural tissues (neuroectoderm), on somites and their derivatives (mesoderm), and transiently on epidermal placodes (somatic ectoderm) (12). We focus the present discussion on cell lineages related to feather histogenesis (15).

L-CAM is continuously present on almost all epidermal cells until they are keratinized (Fig. 9), except in the basilar cells, where it is replaced by N-CAM; such cells later disintegrate. Within single cells at particular sites, the expression of L-CAM occasionally undergoes polarity modulation (13, 23): in placode cells of the skin there is more intense staining by anti-L-CAM on the upper and lower surfaces (the latter facing the N-CAM–positive dermal cells); in barbule-plate cells, there is more intense staining on the sides facing N-CAM–positive axial-plate cells and basilar-layer cells.

The expression of N-CAM is more dynamic than that of L-CAM, and is seen in three lineages (Fig. 9). One lineage proceeds from somite to dermatome to dermal condensation to dermal papilla. The other two lines of expression are on epithelial cells: one appeared as a transient expression of N-CAM in epidermal placode cells and epidermal collar cells, the other was seen as an expression on cells of the marginal plate and axial plate. N-CAM was usually stained homogenously on single cells and in only one situation did it appear to be distributed in a polar fashion: after the axial-plate cells disintegrate, N-CAM branches out extracellularly and coated only the head of the comma-shaped barbule-plate cells.

Borders or interfaces between L-CAM– and N-CAM–positive cell collectives in a CAM couple were found to be associated with important developmental events (Fig. 9, large arrows). The interaction between the placode (L-CAM) and dermal condensation (N-CAM), for example, is accompanied by evagination of the feather bud and the proliferation of the feather epidermis. The interaction between papillar ectoderm (L-CAM) and dermal papilla (N-CAM) is accompanied by the proliferation of the collar and formation of barb ridges. Later, the interaction between the rachidial epidermis (L-CAM) and these cells within the rachidial ridge (N-CAM) is related to the formation of the subridges on the rachis.

Co-expression of L- and N-CAM in a single cell was observed in two situations (Fig. 9). The first was at sites where cells formed blastemata, e.g., in the placode and collar, and in the pulp epithelium and pulp cap. The second was in cells at particular sites at which differential expression of the CAMs occurred, e.g., in barb-ridge epithelia that were newly generated from the collar where L-CAM remained at high levels as N-CAM was declining, and in the basilar layer where N-CAM increased in amount while L-CAM was declining.

Basilar layer cells provide an example in which the differentiation pathway for a gene product other than CAM is modulated with respect to adhesive function. These cells show a switch of CAM expression from L- to N-CAM, while a coordinative switch also occurs so that the cells eventually are not keratinized. Determination of the levels of control of these differentiation events can now be carried out using newly available cDNA probes for N- (24) and L-CAM (25).

In previous studies, N-CAM was found on the cell membrane. In the feather, extracellular N-CAM was observed in the neighborhood regions of the marginal plates and axial plates after cells comprising these structures disintegrate. N-CAM was seen to branch out from the axial-plate cells, and was present between the keratinizing barbule plates, and between the barbule plates and the feather sheath. Another possible location is the interface between epidermal placode and dermal cells, where a sharp line was brightly stained with N-CAM (Fig. 3*d′* of accompanying paper [16]). It is important to stress that extracellular CAMs localized in intercellular

FIGURE 4 Early barb-ridge formation (15, 16), high power view. Cross sections of barb ridges from early to late stages (from *a* to *d*) are double stained with anti-L-CAM (*a–d*) and anti-N-CAM (*a′–d′*) and are shown with their phase-contrast images (*a″–c″*). Dorsal side of the feather is toward the right and the pulp cavity (*p*) is at the bottom of each panel. (*a–a″*) Junction between the stratified feather epithelia (e) and the barb ridges (*br*). The basilayer (*bl*) forms even before the cleavage takes place, and L-CAM staining on this layer is getting fainter. (Arrows point to the valleys.) The smallest ridge that can be recognized is composed of about 20 barb epithelial cells and 20 basilar-layer cells in 10-μm cross sections. *fe*, follicular epidermis. (*b–b″*) More mature stage. The randomly oriented barb epithelial cells start to organize into the barbule plate (*bp*). N-CAM begins to appear on the basilar-layer cells in the valley, spreads bilaterally toward the tip of the ridges, and is more prevalent on the dorsal than the ventral side of the ridge. (*c–c″*) Junction between the barb ridge and the rachidial ridge (*rc*). N-CAM expression on the basilar layer has extended cell by cell (border of expression is pointed to by arrowheads) and the two basilar layers start to "zip" in from the valley (curved arrow). Axial-plate cells (*ap*) appear but are negative for N-CAM at this stage. No difference in L-CAM staining intensity is apparent on the basilar layer before and after the expression of N-CAM. Note that there is a half ridge (on the right) that merges with the rachis. The orientation of cells in the rachis appears disorderly in contrast to those in the barbule plates, and such cells express low amounts of N-CAM. (*d* and *d′*) Marginal plate (*mp*) formation continues. N-CAM appears in the axial plate, extending from the base toward the tip, with newly generated axial-plate cells still negative for N-CAM (small arrow). L-CAM staining on the barbule-plate cells appears to be brighter on the two short sides of these cells facing the axial and marginal plates. (*d″*) Antifibronectin shows continuous and homogenous staining over the pulp side of the basilar layer. Bar, 25 μm; × 325.

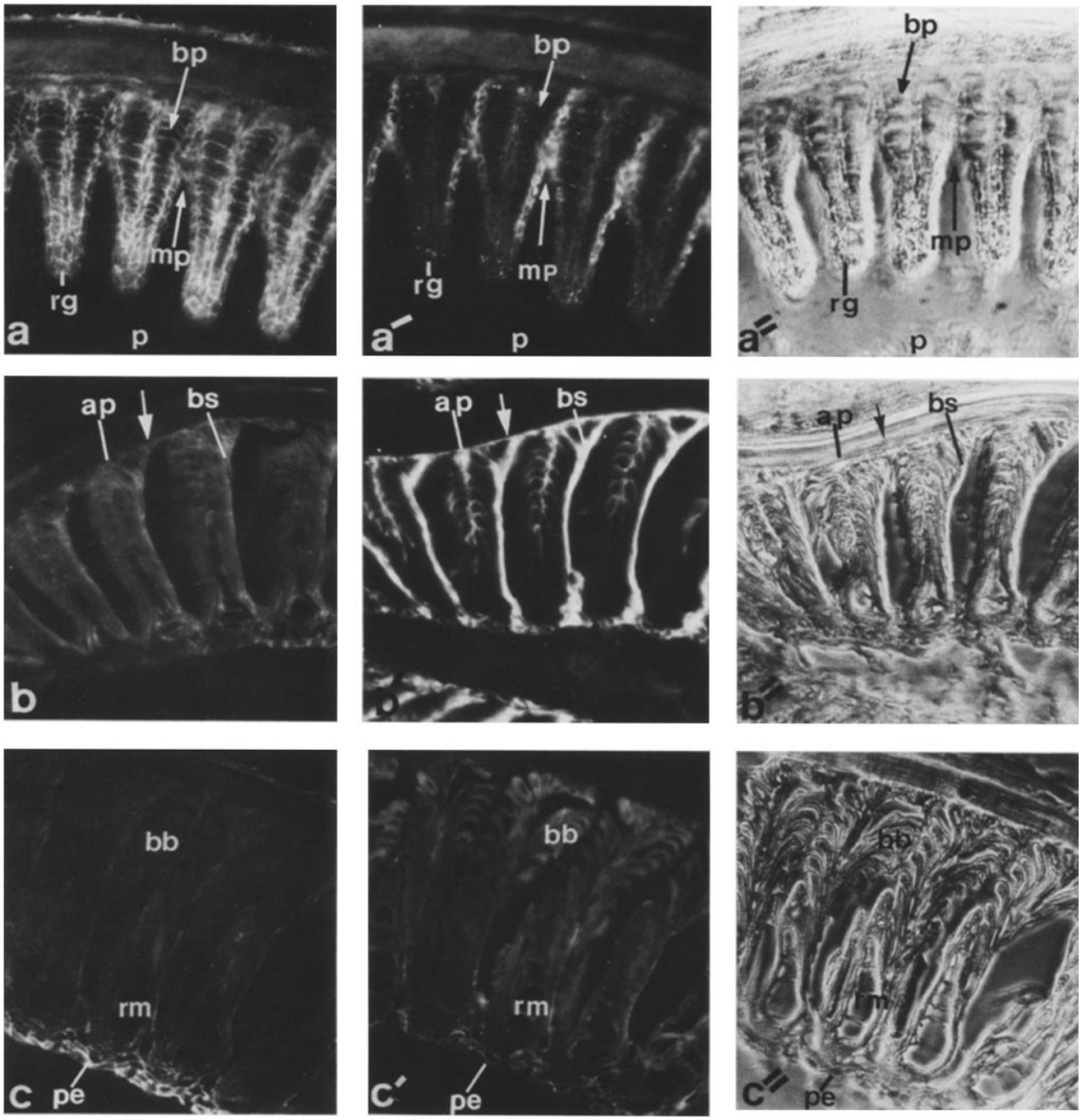

FIGURE 5 Late barb-ridge formation, continuation of Fig. 4. (*a–a″*) Barb ridges elongate as new cells are generated in the ramogenic column (*rg*) at the tip of the ridge. *bp*, barbule plate; *mp*, marginal plate. (*b–b″*) The marginal plate cells have disintegrated, leaving an acellular barb septum (*bs*) that is N-CAM-positive. The axial-plate cells (*ap*) have also disintegrated, leaving a branched distibution pattern in between the keratinizing barbule-plate cells and an N-CAM-positive membrane peripheral to the barb base (small arrow). (*c–c″*) N-CAM-positive barb septa and axial plates have disappeared. Keratinized barbules (*bb*) separate from each other, but remain connected to the ramus (*rm*). *pe*, pulp epithelium. Bar, 25 μm; × 325.

spaces were not co-localized with SAMs or basement membrane.

Pattern Formation: Periodicity within Feathers

Feathers provide an excellent example of pattern formation (26), both because a hexagonal pattern of feathers occurs within pterylae (14, 15) and because a repetitive pattern of barbs and barbules occurs within each feather (15, 17). As described in the previous paper (16), the feather pattern in pterylae within the skin is correlated with the periodic appearance of N-CAM in dermal condensations. Here, we consider periodicity within the feather, in particular the barb pattern that results from the periodic formation of marginal plates, and the barbule pattern that results from periodic formation of the branching axial plates (15, 17). In both cases, CAM-couples or N-linked and L-linked cell collectives that appear in cycles appear to play a key role.

To explain these periodic patterns, it is necessary to under-

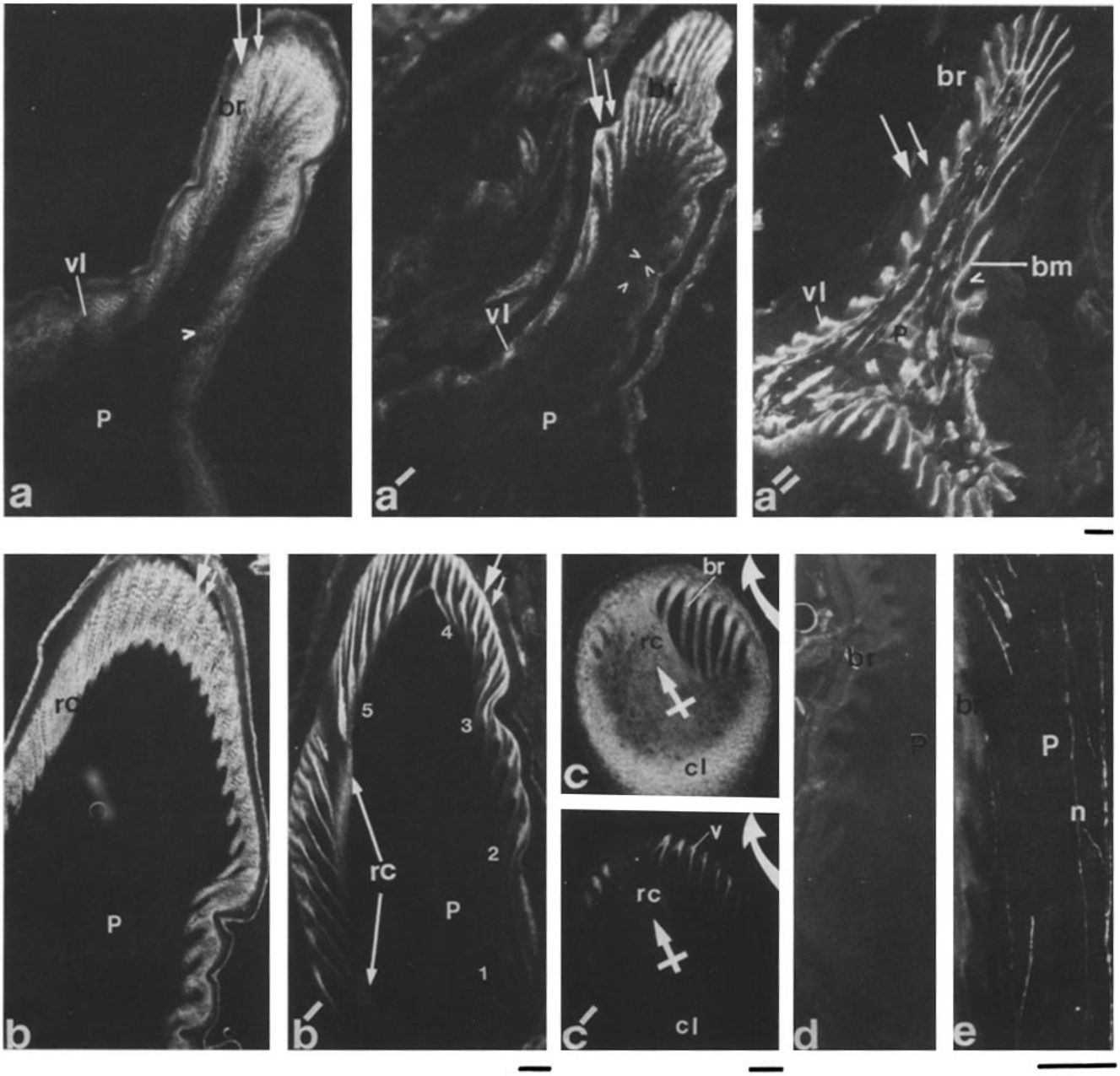

FIGURE 6 Barb-ridge formation (15) in oblique (*a–a''*, *c*, and *c'*) and longitudinal (*b*, *b'*, *d*, and *e*) sections. Skin from the wing of a 5-wk-old chicken was used. (*a–a''*) Neighboring sections are stained with anti-CAMs (*a*, L-CAM; *a'*, N-CAM) and antilaminin (*a''*). Staining with antifibronectin showed the same pattern as laminin. L-CAM and laminin show complementary images: L-CAM is on all the barb-ridge epithelia (*br*), while the boundary facing the pulp (*p*) inside is marked by a basement membrane (*bm*) that is laminin-positive. N-CAM appears within epithelia alternately in the marginal plates (big arrow) and the axial plates (small arrow), but not on the tips of newly formed ridges (arrowheads). *vl*, valley between ridges. (*b* and *b'*) Successive junctions between barb ridges and rachis along the longitudinal axis of the feather are stained with anti-L-CAM (*b*) and anti-N-CAM (*b'*). Feather base is toward the bottom of the panel. A view of the left side of the rachidial ridge shows that barb ridges are periodically connected to this structure (*rc*) at an angle (~30° at this section). The right side of the feather shows the base-to-tip maturation gradient of barb-ridge formation with numbers referring to the stages shown in Fig. 2. N-CAM is stained more intensely on the distal than the proximal sides of the barb ridges. (*c* and *c'*) Relationship among the collar (*cl*), barb ridge, and rachis. Oblique sections are double-stained with anti-L-CAM (*c*) and anti-N-CAM (*c'*). The axis of the feather is indicated by the arrow with crossbar. Section plane on the right side passes closer to the rachis than that on the left side. New barb ridges are generated from the collar at an angle (~60° with the base); as the rachis elongates, the ridges will be "dragged" in to become inserted on the rachis instead of on the collar base. Curved arrow indicates the direction of maturation of barb ridges. Section plane on the left passes mostly through epithelia that have not yet cleaved, except for those shown in the tangentially sectioned valleys. On the right, N-CAM appears on the tip of the developing valleys but is not yet present in the junctions between barb ridges and rachis. N-CAM is also faintly present on the collar. (*d*) Anti-N-CAM staining in the basilar layer and axial plate is completely neutralized by absorption of the antibodies with brain N-CAM. (*e*) Neuron-specific anti-Ng-CAM stains nerves (*n*) that run longitudinally in the pulp cavity. Bar, 100 μm. (*a–c'*) × 50; (*d* and *e*) × 126.

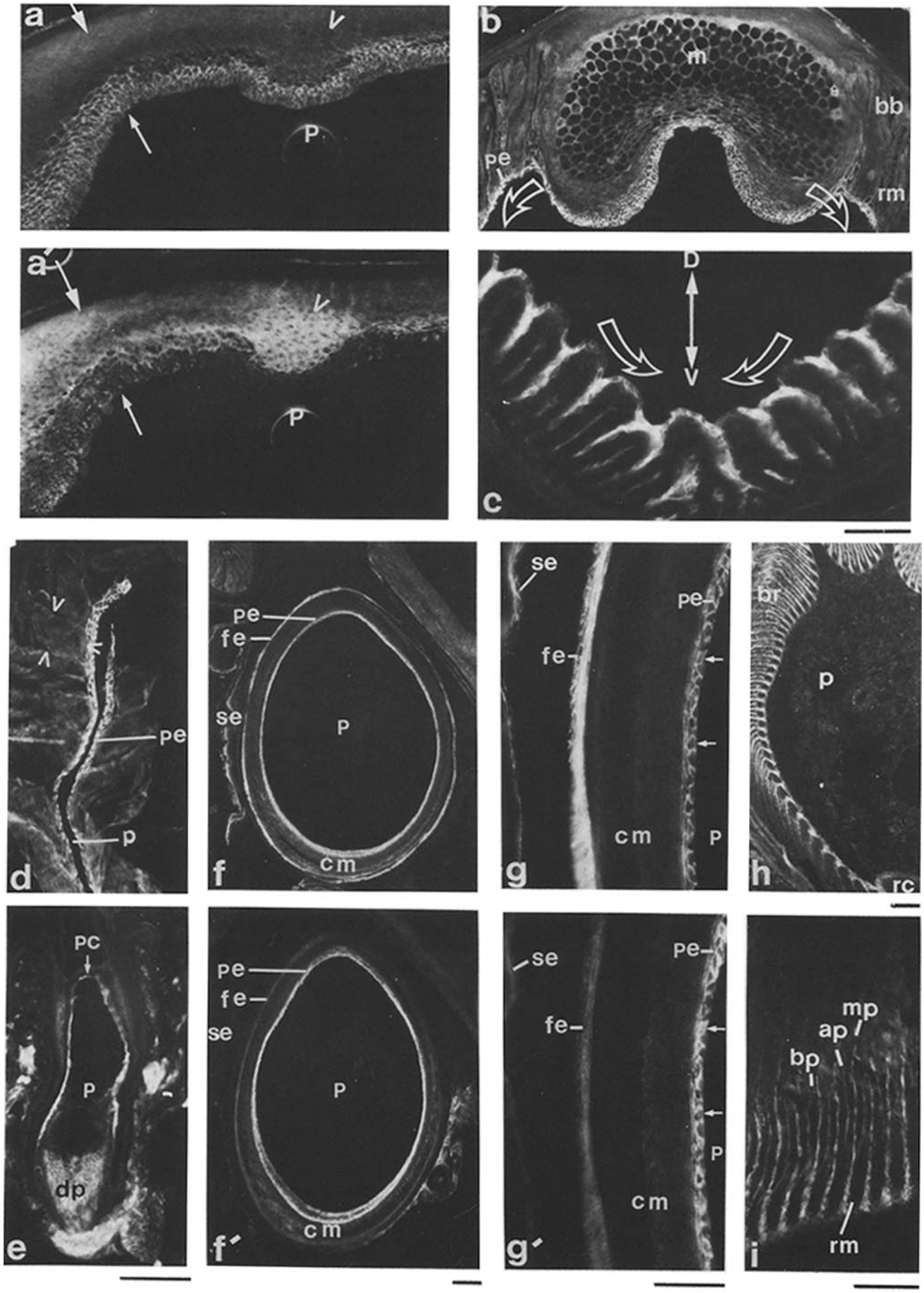
a
v
P
b
m
bb
pe
rm
a'
v
P
c
D
V
d
v
pe
p
f
pe
fe
se
P
cm
g
se
pe
fe
cm
P
h
br
p
rc
e
pc
P
dp
f'
pe
fe
se
P
cm
g'
se
pe
fe
P
cm
i
mp
ap
bp
rm

stand the precise order of structure-forming events and the nature of the signals that initiate them. The order of events is more apparent within the feather filament than in the dermal condensations described in the previous paper (16), because a filamentous conformation is equivalent to a two-dimensional structure, affording the opportunity to observe a single cell when a particular CAM was expressed. In the present study, it was found that the early temporal order in marginal plate formation was (*a*) the appearance of a layer of stratified epithelial cells expressing L-CAM, (*b*) the formation of the one cell thick basilar layer on the pulp side of the stratified epithelium (which still remained L-CAM–positive) (*c*) the initiation of clustering of the epithelial cells to form barb ridges, and (*d*) the appearance of N-CAM in a single basilar cell in the valley between barb ridges, with later propagation of expression cell by cell to form the marginal plate. For the axial plate, the comparable order was (*a*) the appearance of a group of randomly oriented barb epithelial cells (a process similar to step *c* above) and (*b*) the formation of two rows of rectangular barbule-plate cells flanking a string of spindle-shaped axial-plate cells—both of which cells expressed L-CAM—and, finally, (*c*) the appearance of N-CAM in a single axial-plate cell at the base of the barb ridges, with later propagation cell by cell to form the N-CAM–positive axial plate. It is important to note that in both the orders for marginal-plate and axial-plate formation the patterned arrangement of cells expressing L-CAM preceded the initial appearance of N-CAM.

In addition to more elaborate spatial periodicity, the other major pattern change in the adult feather as compared to the nestling feather is the change from a radially symmetrical to a bilaterally symmetrical arrangement of barbs (15, 17). This symmetry change is achieved via two major steps: first, the fusion of barb ridges into the rachidial ridge, and, second, the formation of an angle between the rachidial ridge and the barb ridges (15, 17). The formation of this angle can be explained by the simultaneous coupling of periodic waves of barb-ridge formation along a horizontal axis with periodic waves of barb-ridge formation along a longitudinal axis. A signaling mechanism involving N-CAM/L-CAM couples similar to that proposed to explain the periodicity of initial inductions of feather placodes in pterylae (16) could result in such waves. This is an attractive hypothesis because of its testability in vitro (27) with anti-CAM antibodies and its generality in explaining periodicity both among and within feathers.

Different Roles of CAMs and SAMs in Feather Morphogenesis

Unlike the CAM couples, the SAMs, exemplified here by fibronectin and laminin, are not seen in periodic distributions nor are they localized at sites of induction. SAMs therefore do not appear to play the same role in the morphogenesis of the feather as do the primary CAMs. Instead, they are likely to play important adjunct roles in separating germ layer derivatives for certain periods of time, in providing substrates for cell movement, and in stabilizing morphological patterns (21, 28–30). For example, it is known that the epidermal-dermal junction that is rich in collagens breaks down at the sites of placode induction (28); this may be a prelude for the interactions between collectives of dermal cells linked by N-CAM with collectives of epidermal cells linked by L-CAM. While fibronectin and collagen still occur in the feather bud, they do not form a membrane to separate the two germ layers (28). Fibronectin is enriched in the ventral part of the growing bud (28), but, as shown here, is completely excluded from mature dermal papillae. In contrast, N-CAM is enriched in the dorso-basal part of the growing feather bud dermis and is strongly expressed in the well-confined dermal papilla. In sites such as the feather bud, fibronectin may allow cell migration, whereas N-CAM may impede it through its role in mediating intercellular adhesion.

During induction within the dermal papilla, fibronectin and laminin fail to form a basement membrane between the dermis and epidermis (16). During barb-ridge formation, however, they do form a homogeneously stained and continuous basement membrane that separates the basilar layer and barb epithelia from pulp cells. This membrane does not show the accentuated periodic staining seen for N-CAM, nor are

FIGURE 7 Rachis and pulp epithelium (15). Sections of feathers from 5-wk-old chicken wing are stained with anti-L-CAM (*a*, *b*, *d*, *f*, and *g*) and anti-N-CAM (*a'*, *c*, *e*, *f'*, *g'*, *h*, and *i*). *a* (anti-L-CAM) and *a'* (anti-N-CAM), early rachis formation at stages corresponding to Fig. 3*c*. The double staining shows three kinds of cells in the rachidial ridge: undifferentiated cells positive for both L- and N-CAM (large arrow), epithelial cells lining the pulp cavity positive for L-CAM (small arrow), and cells just under these epithelial cells positive for N-CAM (arrowhead). The last kind of cell is particularly concentrated under the evaginated ridges of the rachis. *p*, pulp cavity. (*b*) Anti-L-CAM. Late rachis formation at a stage corresponding to Fig. 3*e'*. The undifferentiated cells in the periphery have keratinized, the epithelial cells are still L-CAM positive and become part of the pulp epithelium (*pe*). Many cells in the center of rachidial ridge have vacuolated to form the medulla (*m*) of the rachis. *rm*, ramus; *bb*, barbule. (*c*) Anti-N-CAM. The two laterally propagating ridge forming waves (curved arrows) from the rachis meet at the ventral point. Note the mirror symmetry around the dorsal-ventral (*D–V*) axis. (*d*) Anti-L-CAM. Pulp epithelium (*pe*). Longitudinal section of the feather shaft. The keratinized barbs (one barb is surrounded by arrowhead) have split. Pulp epithelium, positive for both CAMs, still lines the pulp cavity (*p*), but this cavity will soon disappear when the pulp epithelium disintegrates. (*e*) Anti-N-CAM. Longitudinal section of the feather base. Most of the pulp has been absorbed and the pulp epithelium has retracted to become the pulp cap (*pc*) that encloses the remnant pulp cavity. *dp*, dermal papilla. (*f* and *f'*) Anti-L-CAM and anti-N-CAM, respectively. Cross sections of the feather base. The collar has now keratinized into a cylindrical calamus (*cm*) into which the rachis inserts. Among the three cell types of epithelial origin, the pulp epithelium is both N-CAM- and L-CAM–positive, but the follicular epidermis (*fe*) and skin epidermis (*se*) are L-CAM–positive only. (*g* and *g'*) Anti-L-CAM and anti-N-CAM, respectively. Double staining to show that single cells in the pulp epithelium are indeed both L-CAM- and N-CAM–positive (arrow), and that cells in the follicular and skin epidermis are not. (*h* and *i*) Anti-N-CAM. Developing barb ridges from an adult chicken, 6-mo-old. The barb ridge is at least 10 times longer than the adult feathers of earlier molting cycles (compare with Fig. 3*d*), also note that the heights of barb ridges are uneven along the feather perimeter. Bar, 100 μm. (*a–e*, *g*, *g'*, and *i*) × 126; (*f*, *f'*, and *h*) × 50.

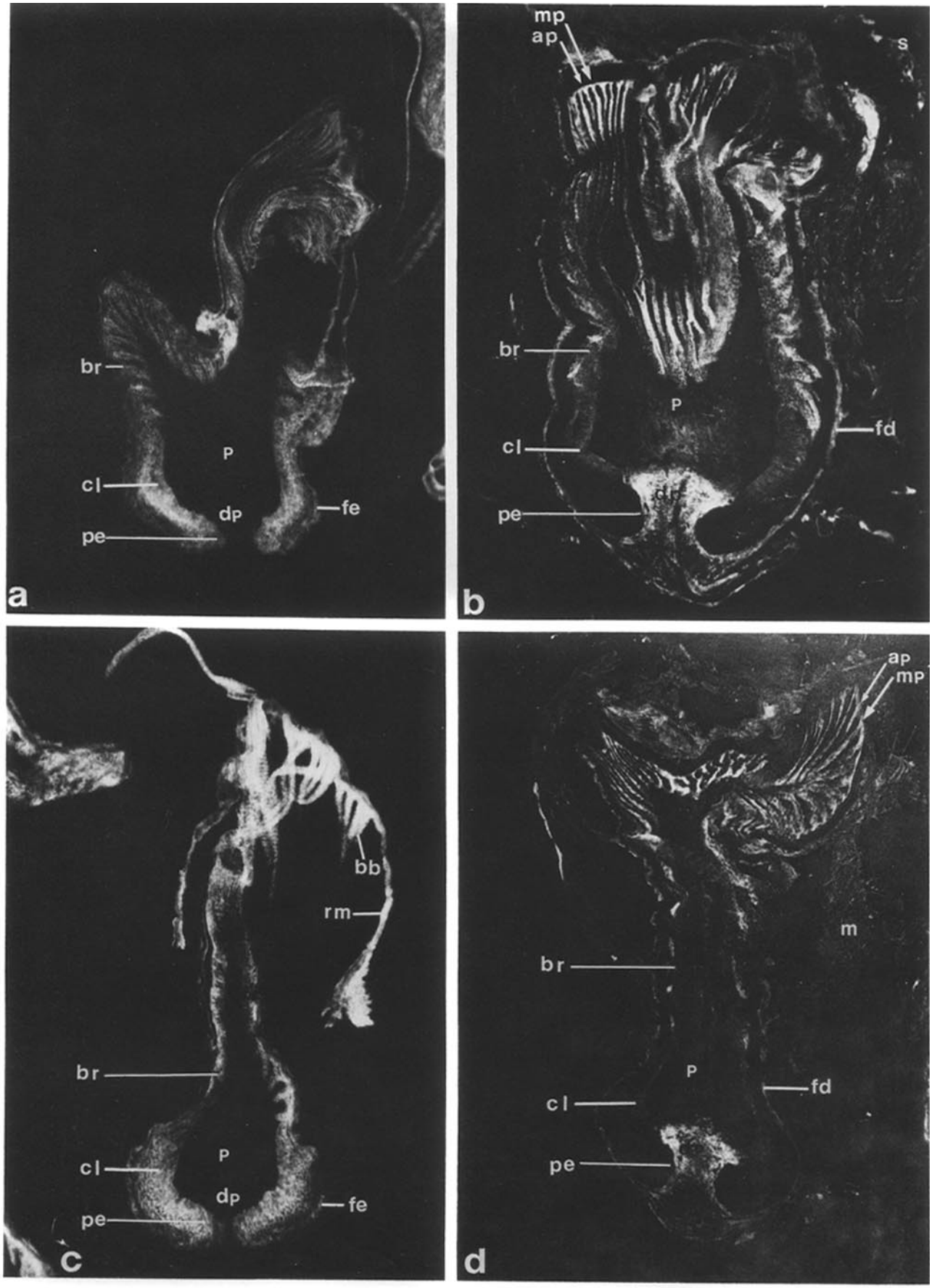

FIGURE 8 Longitudinal sections of whole developing feather follicles from a newly hatched chicken wing, summarizing the entire sequence of expression of L-CAM (*a* and *c*) and N-CAM (*b* and *d*) during adult feather histogenesis. The bilateral branching of follicles in *a* and *d* possibly reflects the formation of feather and after-feather (see reference 15). Proceeding from the dermal papilla (*dp*), the epithelial cells develop from papillar ectoderm (*pe*) to collar (*cl*) to barb ridges (*br*) and then to rami (*rm*) and barbules (*bb*), reflecting temporal developmental stages on a spatial array ranging from base to tip. *ap*, axial plate; *fd*, follicular dermis; *fe*, follicular epidermis; *m*, muscle; *mp*, marginal plate; *p*, pulp cavity; *s*, skin. Bar, 100 μm; × 50.

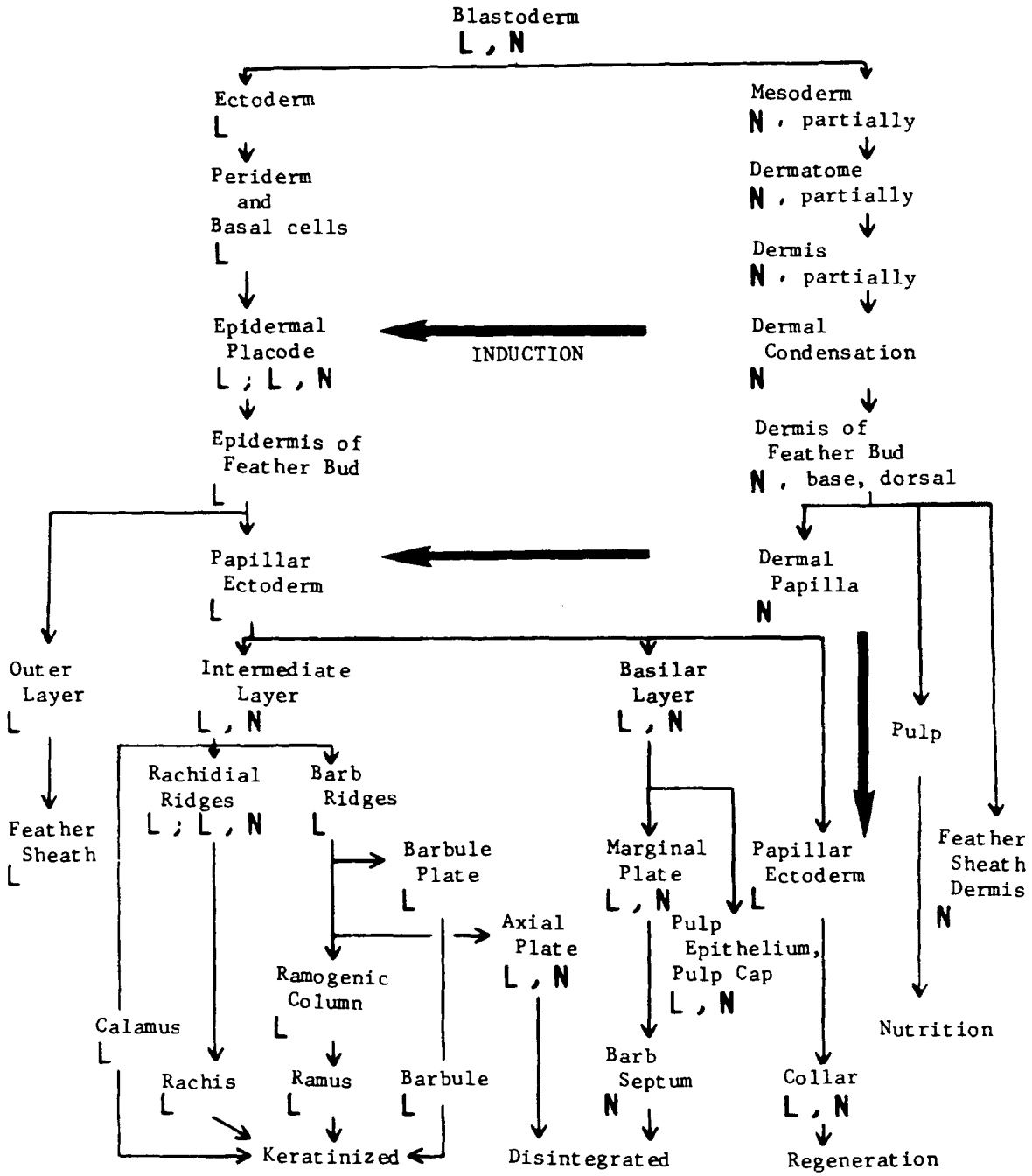

FIGURE 9 The expression of L-CAM (*L*) and N-CAM (*N*) during feather morphogenesis is mapped onto the lineage of feather tissues (1, 15). Three bold arrows represent induction events; other arrows represent tissue lineage.

SAMs observed between the barb epithelia and basilar layer or the barb epithelia and the axial-plate cells.

Recombination experiments have shown that the feather pattern on the skin as well as that of the rachis and the barbs depends upon the mesoderm, but that the barbule pattern (number and shape of each barbule) depends upon the ectoderm (14, 31). The present experiments show that CAM couples for feather placodes and for the rachis and barb patterns are derived from mesoderm (N) and ectoderm (L), whereas the new couples in the axial plates arise completely from ectoderm, which can express both L- and N-CAM. These findings are in accord with the conclusion that the feather sites and the rachis and barb patterns occurring at the interfaces between dermis and epidermis are dependent on mesoderm (for the feather sites, these interfaces are the dermal condensation and epidermal placode; for the rachis and barb, they are the dermal papilla and the epidermal collar), while the barbule patterns and numbers that occur within the epidermis are dependent on ectoderm (axial plate/barbule plate). All of these observations suggest that CAM couples, rather than germ-layer origins or segregation of germ-layer derivatives by basement membranes, may play a more important role in initiating pattern formation at different levels.

CAM Couples and Regulation of Primary Processes

It is important to consider the functional significance of the

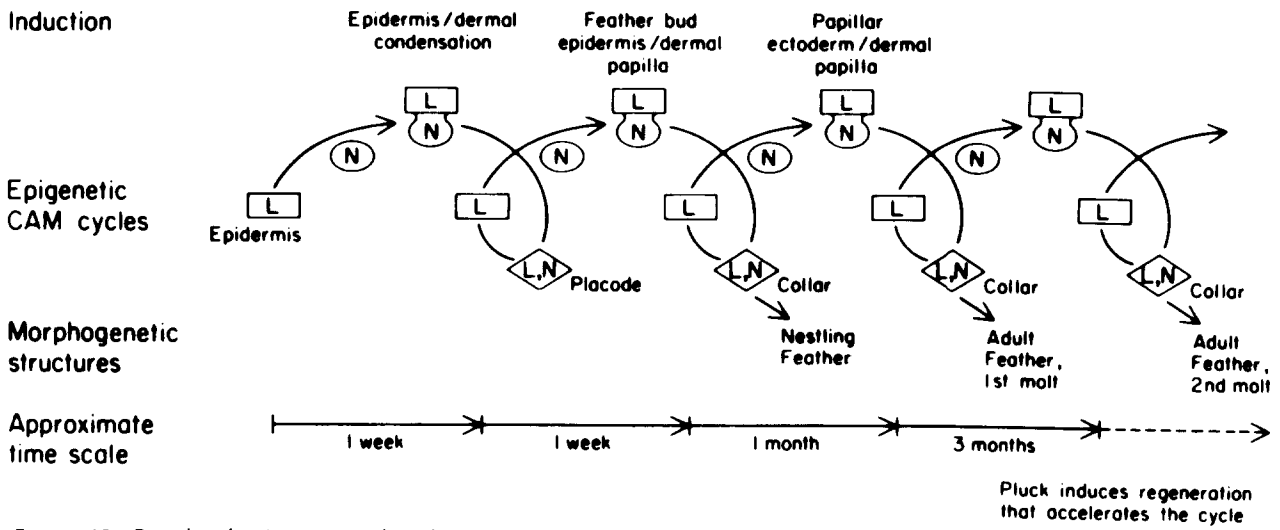

FIGURE 10 Postulated epigenetic cycles of CAM appearances in feather morphogenesis. Targets of induction are represented by rectangles; inducers are represented by ellipses; the names of the associated tissues in each cycle are listed on top. Results of the induction are represented by diamonds. Morphogenetic structures generated in part by expression of differentiation products other than CAMs are pointed to by arrows branching out from the epigenetic cycles. *L*, L-CAM; *N*, N-CAM. Examples of other related epigenetic CAM cycles in other regions that ultimately contribute to feather morphogenesis are: blastoderm (*L*, *N*) proceeding to primary mesenchyme (no *N*) and to somite (*N*); somite (*N*) proceeding to dermatome (no *N*) to migrating cells (no *N*) to dermal condensation (*N*).

remarkable repetitious appearance of CAM couples in the various morphogenetic process of feather formation. In the regulator hypothesis (4), it has been suggested that the expression of CAMs may act as a major early event in the sequence of control of other primary processes. For the feather, these processes include proliferation (in feather bud epidermis, collar, ramogenic column, rachidial column, and dermal condensations), movement (in dermal condensations and barb-ridge and barbule-plate formation), death (in marginal and axial plate), and differentiation (as seen in the keratinization of the rachis, ramus, and barbule). N-CAM/L-CAM couples appear at each of the strategic positions and time points (Fig. 10); the consistency of their appearance and the known adhesive function of the CAMs suggest that they are instrumental in these morphogenetic events. For example, when couples appear at the sites of placode induction, the epithelia undergo active proliferation; after couples appear in the basilar- and axial-plate epithelia, the cells die without keratinizing. Combinatorial rearrangements of such processes during evolution could be used to build up complex patterns with different morphological consequences (4).

How can such processes be coordinated during ontogeny? It is pertinent to note that in induction at different sites, there is a consistent cyclic expression of CAMs (Fig. 10). Each cycle consists of the apposition of an N-CAM–positive cell collective with an L-CAM–positive cell collective, and results in a new structure that is both N-CAM– and L-CAM–positive. These cells can then differentiate as well as go through another CAM cycle. The cell types that form these cell collectives and the morphogenetic structures that result from successive cycles can vary (Fig. 10), and this variance depends upon the expression of genes for differentiation products other than CAMs. Epigenetic alterations in the schedules of CAM cycles and of gene expression for other proteins could lead to varieties in shapes and sizes of tissue structures.

The direct influence of cycles of CAM gene expression and surface modulation on induction events and the correlated expression of other gene products remains to be proven by experimental manipulations, including perturbation of cell interactions with anti-CAM antibodies and exploration of the mechanisms of CAM gene expression with cDNA probes (24, 25). Even at the present descriptive stage, however, the results raise the possibility that small changes in the effects of a few regulatory genes, such as those governing CAM expression, could lead to large phenotypic variation in feathers. Because of its genetic parsimony and its dependence on primary processes of development, this hypothesis is consistent with the idea that natural selection acting on birds with particular feather forms (32) could result in relatively rapid alterations in different species during evolution. A similar argument has been applied to other organs (4, 13) and the confirmed appearance of CAM couples at many morphogenetic sites (22) is also consistent wtih this point of view.

We thank Ms. Alison Schroeder for her excellent technical assistance.

This work was supported by U.S. Public Health Service grants AM-04256, HD-09635, and HD-16550.

Received for publication 28 March 1985, and in revised form 7 May 1985.

REFERENCES

1. Carlson, B. M. 1981. Patten's Foundations of Embryology. McGraw-Hill Book Co., New York. 1–672.
2. DeHaan, R. L., and H. Ursprung, editors. 1964. Organogenesis. Holt, Rinehart and Winston, New York. 1–804.
3. Slack, J. M. W. 1983. From Egg to Embryo. Cambridge University Press, New York. 1–241.
4. Edelman, G. M. 1984. Cell adhesion and morphogenesis: the regulator hypothesis. *Proc. Natl. Acad. Sci. USA* 81:1460–1464.
5. Edelman, G. M. 1983. Cell adhesion molecules. *Science (Wash. DC)*. 219:450–457.
6. Edelman, G. M. 1984. Modulation of cell adhesion during induction, histogenesis, and perinatal development of the nervous system. *Annu. Rev. Neurosci.* 7:339–377.
7. Horwitz, A., K. A. Knudsen, C. H. Damsky, C. Decker, and N. T. Neff. 1984. Adhesion-related integral membrane glycoproteins identified by monoclonal antibodies. *In* Monoclonal Antibodies and Functional Cell Lines. R. H. Kennett, K. B. Bechtel, and T. J. McKearn, editors. Plenum Publishing Corp., New York. 103–118.
8. Brackenbury, R., J.-P. Thiery, U. Rutishauser, and G. M. Edelman. 1977. Adhesion among neural cells of the chick embryo. I. An immunological assay for molecules involved in cell-cell binding. *J. Biol. Chem.* 252:6835–6840.
9. Gallin, W. J., G. M. Edelman, and B. A. Cunningham. 1983. Characterisation of L-

CAM, a major cell adhesion molecule from embryonic liver cells. *Proc. Natl. Acad. Sci. USA.* 80:1038–1042.
10. Grumet, M., and G. M. Edelman. 1984. Heterotypic binding between neuronal membrane vesicles and glial cells is mediated by a specific cell adhesion molecule. *J. Cell Biol.* 98:1746–1756.
11. Edelman, G. M., W. J. Gallin, A. Delouvée, B. A. Cunningham, and J.-P. Thiery. 1983. Early epochal maps of two different cell adhesion molecules. *Proc. Natl. Acad. Sci. USA.* 80:4383–4388.
12. Thiery, J.-P., J.-L. Duband, U. Rutishauser, and G. M. Edelman. 1982. Cell adhesion molecules in early chicken embryogenesis. *Proc. Natl. Acad. Sci. USA.* 79:6737–6741.
13. Thiery, J.-P., A. Delouvée, W. J. Gallin, B. A. Cunningham, and G. M. Edelman. 1984. Ontogenetic expression of cell adhesion molecules: L-CAM is found in epithelia derived from the three primary germ layers. *Dev. Biol.* 102:61–78.
14. Sengel, P. 1976. Morphogenesis of Skin. Cambridge University Press, New York.
15. Lucas, A. M., and P. R. Stettenheim. 1972. Avian anatomy. Integument. Part I and Part II. *In* Agriculture Handbook. Agricultural Research Service, U.S. Department of Agriculture, Washington D.C. 362:1–750.
16. Chuong, C.-M., and G. M. Edelman. 1985. Expression of cell adhesion molecules in embryonic induction. I. Morphogenesis of nestling feathers. *J. Cell. Biol.* 101:1009–1026.
17. Hosker, A. 1936. Studies on the epidermal structures of birds. *Philos. Trans. R. Soc. Lond. B Biol. Sci.* 225:143–188.
18. Wang, H. 1943. The morphogenetic function of the epidermis and dermal components of the papilla in feather regeneration. *Physiol. Zool.* 16:325–350.
19. Hoffman, S., B. C. Sorkin, P. C. White, R. Brackenbury, R. Mailhammer, U. Rutishauser, B. A. Cunningham, and G. M. Edelman. 1982. Chemical characterization of a neural cell adhesion molecule purified from embryonic brain membranes. *J. Biol. Chem.* 257:7720–7729.
20. Haake, A. R., G. König, and R. H. Sawyer. 1984. Avian feather development: relationships between morphogenesis and keratinization. *Dev. Biol.* 106:406–413.
21. Hay, E., editor. 1981. Cell Biology of Extracellular Matrix. Plenum Publishing Corp., New York. 1–147.
22. Crossin, K. L., C.-M. Chuong, and G. M. Edelman. 1985. Expression sequences of cell adhesion molecules. *Proc. Natl. Acad. Sci. USA.* In press.
23. Edelman, G. M. 1976. Surface modulation in cell recognition and cell growth. *Science (Wash. DC).* 192:218–226.
24. Murray, B. A., J. J. Hemperly, W. J. Gallin, J. S. MacGregor, G. M. Edelman, and B. A. Cunningham. 1984. Isolation of cDNA clones for the chicken neural cell adhesion molecule. *Proc. Natl. Acad. Sci. USA.* 81:5584–5588.
25. Gallin, W. J., E. A. Prediger, G. M. Edelman, and B. A. Cunningham. 1985. Isolation of a cDNA clone for the liver cell adhesion molecule (L-CAM). *Proc. Natl. Acad. Sci. USA.* 82:2809–2813.
26. Malacinski, G. M., and S. V. Bryant, editors. 1984. Pattern Formation, a Primer in Developmental Biology. Macmillan Publishing Co., New York. 1–626.
27. Novel, G. 1973. Feather pattern stability and reorganization in cultured skin. *J. Embryol. Exp. Morphol.* 30:605–633.
28. Mauger, A., M. Demarchez, D. Herbage, J.-A. Grimaud, M. Druguet, D. Hartmann, and P. Sengel. 1982. Immunofluorescent localization of collagen types I and III, and of fibronectin during feather morphogenesis in the chicken embryo. *Dev. Biol.* 94:93–105.
29. Kitamura, K. 1981. Distribution of endogenous β-galactoside-specific lectin, fibronectin and type I and III collagens during dermal condensation in chick embryos. *J. Embryol. Exp. Morphol.* 65:41–56.
30. Sengel, P. 1985. Role of extracellular matrix in the development of skin and cutaneous appendages. *In* Developmental Mechanisms Normal and Abnormal. Alan R. Liss, Inc., New York. 123–135.
31. Dhouailly, D. 1984. Specification of feather and scale patterns. *In* Pattern Formation, a Primer in Developmental Biology, G. M. Malacinski and S. V. Byrant, editors. Macmillan Publishing Co., New York. 581–601.
32. Burton, M., editor. 1980. The New Larousse Encyclopedia of Animal Life. Bonanza Books, New York. 331–467.